Scattering of co-current surface waves on an analogue black hole

Léo-Paul Euvé, Scott Robertson, Nicolas James, Alessandro Fabbri, Germain Rousseaux

Scattering of Co-Current Surface Waves on an Analogue Black Hole

Léo-Paul Euvé,[1] Scott Robertson,[2] Nicolas James,[3] Alessandro Fabbri,[4,5,2] and Germain Rousseaux[6]
[1]Laboratoire de Physique et Mécanique des Milieux Hétérogènes (UMR 7636), ESPCI, Université PSL, CNRS, Sorbonne Université, Université Paris Diderot, 10 rue Vauquelin, 75321 Paris Cedex 05, France
[2]Université Paris-Saclay, CNRS/IN2P3, IJCLab, 91405 Orsay, France
[3]Laboratoire de Mathématiques et Applications (UMR 7348), CNRS—Université de Poitiers, 11 Boulevard Marie et Pierre Curie—Téléport 2–BP 30179, 86962 Futuroscope Chasseneuil Cedex, France
[4]Departamento de Física Teórica and IFIC, Centro Mixto Universidad de Valencia—CSIC, C. Dr. Moliner 50, 46100 Burjassot, Spain
[5]Centro Fermi—Museo Storico della Fisica e Centro Studi e Ricerche Enrico Fermi, Piazza del Viminale 1, 00184 Roma, Italy
[6]Institut Prime (UPR 3346), CNRS—Université de Poitiers—ISAE ENSMA, 11 Boulevard Marie et Pierre Curie—Téléport 2–BP 30179, 86962 Futuroscope Chasseneuil Cedex, France

(Received 5 July 2019; revised manuscript received 20 November 2019; accepted 12 March 2020; published 7 April 2020)

We report on what is to our knowledge the first scattering experiment of surface waves on an accelerating transcritical flow, which in the analogue gravity context is described by an effective spacetime with a black-hole horizon. This spacetime has been probed by an incident co-current wave, which partially scatters into an outgoing countercurrent wave on each side of the horizon. The measured scattering amplitudes are compatible with the predictions of the hydrodynamical theory, where the kinematical description in terms of the effective metric is exact.

DOI: 10.1103/PhysRevLett.124.141101

Recent years have witnessed an explosion of interest in analogue gravity [1,2]. This newly emergent field builds on Unruh's insight of 1981 [3] that, using the mathematical equivalence between wave propagation in curved spacetimes on the one hand and in condensed matter systems on the other, one can realize an analogue black hole in the laboratory and test Hawking's prediction that black holes emit radiation [4,5]. In this context, an analogue black hole is engendered by an accelerating flow which becomes supersonic. The point where the flow crosses the speed of sound is the (acoustic) horizon for sound waves, in analogy with the (event) horizon for light at a gravitational black hole. Because wave propagation close to the horizon is equivalent in the two cases, the Hawking effect, which is derived from purely kinematical considerations, should be present also in the analogue system. This prediction has been the main driving force behind the analogue gravity program since its inception, with experimental studies in a wide range of physical systems, such as nonlinear optics [6–9], exciton-polaritons [10], and Bose-Einstein condensates [11–13].

Surface waves on fluids provide another example of an analogue system [14,15]. Consider a rectangular flume oriented along the x direction, containing a water flow which is independent of the transverse coordinate y. In the shallow-water limit $kh \ll 1$ (k being the wave vector and h the depth), the free-surface deformation δh behaves like the canonical momentum of a minimally coupled massless scalar field propagating in the $(2+1)$-dimensional spacetime metric

$$ds^2 = c^2[c^2dt^2 - (dx - vdt)^2 - dy^2]. \tag{1}$$

The metric (1) describes a "spacetime fluid" flowing in the x direction with velocity $v(x)$ and variable "speed of light" $c(x)$. The x-oriented null geodesics of the metric (1) are simply described by $dx/dt = v \pm c$. For waves, this equation gives the motion of characteristics, and is equivalent to the following (linear) dispersion relation whenever v and c are constant:

$$\Omega = \omega - vk = \pm ck, \tag{2}$$

where Ω is the "comoving" frequency measured in the rest frame of the fluid, while ω is the Doppler-shifted frequency measured in the lab frame. We assume the flow is from left to right, i.e., $v > 0$, so that the plus and minus signs in Eq. (2) respectively define waves engaged in *co-* and *countercurrent* propagation. In particular, the total velocity of countercurrent waves is $v - c$, which can take either sign. A *transcritical* flow has $v - c = 0$ somewhere. This point is the (analogue) horizon, marking the boundary between *subcritical* ($v - c < 0$) and *supercritical* ($v - c > 0$) regions. Accelerating flows which pass from subcritical to supercritical have specifically an analogue *black-hole* horizon, with countercurrent waves outgoing on either side.

Matters are complicated by the prefactor of c^2 in Eq. (1), which can be thought of as a conformal factor relating the effective metric to the simpler one in square brackets. In an appropriate coordinate system, this term generates an effective potential [16,17] which scatters co- into countercurrent

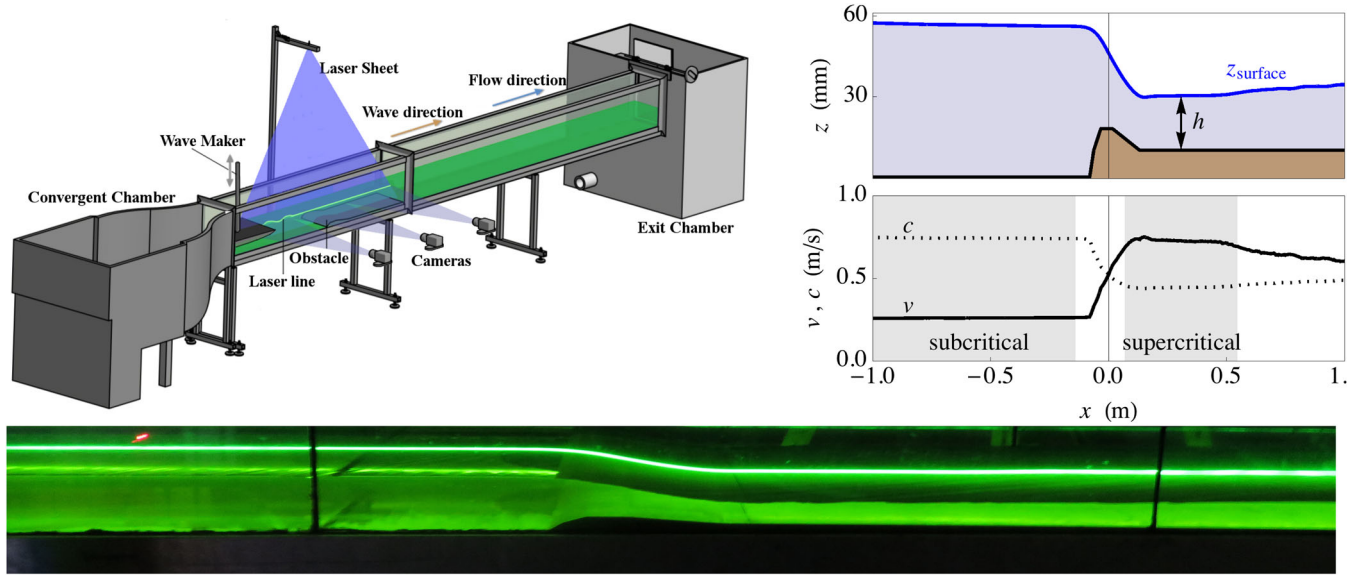

FIG. 1. Experimental setup. On the left is an illustration of the flume, showing the flow direction and the position of the wave maker. On the right are shown the following: (upper) the obstacle on the bottom of the flume and the stationary profile of the surface, found by averaging $z_{\mathrm{surface}}(t,x)$ over time; (lower) the corresponding profiles of v and c [according to Eqs. (3)], with the near-homogeneous regions (where the plane wave decomposition is performed) shaded. The bottom panel shows a photo of the flume, where one sees clearly the variation of the water depth and the laser illuminating the midline. The distance between the black vertical bars is 1 m.

waves and vice versa. The two outgoing countercurrent waves can thus be excited by a co-current wave sent in by a wave maker.

There have been a number of recent experiments aimed at realizing and probing analogue spacetimes of the form (1) seen by surface waves [18–24]. However, these have tended to remain far from the ideal case originally envisaged by Unruh. Most importantly, in none of these experiments was a transcritical flow achieved, so that the corresponding analogue spacetimes did not contain horizons [25]. In such cases, the nontrivial scattering processes analogous to those involved in the Hawking effect can exist only thanks to the presence of short-wave dispersion, which requires the singling out of a preferred frame and thus breaks the analogue of Lorentz invariance. The relevant scattering amplitudes cannot be derived from the spacetime description; in particular, those pertaining to the analogue of the Hawking process do not generally follow the Planck law so central to Hawking's thermal prediction [26,27]. Furthermore, all experiments in 1D settings have focused on decelerating flows, which in the transcritical case would yield analogue white-hole horizons. These are convenient for scattering experiments as they convert incident hydrodynamical (long-wavelength) waves, which are easy to excite, into outgoing dispersive (short-wavelength) waves, which are easy to measure. However, this means that the kinematics of the outgoing modes are not describable using the effective metric formalism alone. Things are further complicated by the ubiquity of undulations (i.e., zero-frequency solutions with finite wave vector) on the downstream sides of decelerating flows [28,29].

Experimental setup.—We have realized, at Institut Pprime of the University of Poitiers, a transcritical flow in a flume analogous to a black-hole spacetime, and performed a scattering experiment on this flow that can be described in terms of the effective metric. The experimental setup and the stationary flow profile are illustrated in Fig. 1. A flume of length 7 m and width 39 cm is used, and on the bottom of the flume is placed a dedicated obstacle with x-dependent height, designed in accordance with well-known principles of hydraulics (set out pedagogically by Walker in [30]). The current is maintained by a PCM Moineau pump. The convergent chamber, containing a honeycomb structure, removes practically all boundary-layer effects and macrovortices, producing a flow velocity profile that (in the upstream region) is approximately constant in both the vertical and transverse directions. At a given flow rate, which is measured by a Promag 55S flow meter to within an error of 0.5%, the stationary flow that results has a particular mean depth profile $h(x)$. The presence of surface waves causes the instantaneous depth to vary in time around this mean.

Measurements were made of the instantaneous vertical position $z_{\mathrm{surface}}(t,x)$ of the water surface along the midline of the flume. A laser sheet, produced by a laser diode (at wavelength 473 nm and power 100 mW) and a Powell lens, was shone through the water, to which had been added fluorescein dye [20,22]. At a suitable concentration ($\sim$20 g/m^3), the dye absorbs the blue laser light and emits green light near the surface (up to a depth of $\sim$5 mm). The laser line produced (see Fig. 1) was recorded by three cameras at regular intervals of $\Delta t \sim 0.1$ s, for a total

duration of 800 s. A subpixel detection algorithm yielded the surface height at each time at a series of positions separated by the constant spacing $\Delta x = 3.4$ mm. From this was subtracted the known height profile of the obstacle in order to get the instantaneous water depth $h(t, x)$. The mean depth $h(x)$ is then found by averaging over time. Assuming the fluid to be irrotational and the surface quasiflat (i.e., $|\partial_x z_{\text{surface}}| \ll 1$), the flow velocity and wave speed are related to the mean depth by

$$v(x) = \frac{q}{h(x)}, \qquad c(x) = \sqrt{gh(x)}, \tag{3}$$

where q is the (constant) flow rate per unit width (measured at 147.4 ± 0.7 cm^2/s) and $g = 9.8$ m/s^2 is the acceleration due to gravity. As seen in the lower right panel of Fig. 1, the realized flow passes from subcritical to supercritical, thus engendering an analogue black-hole horizon at the point where $v = c$.

Surface waves were stimulated by a plunging-type wave maker placed upstream from the obstacle. We performed a series of experimental runs for a range of frequencies at three different wave maker amplitudes: $A_{\text{wm}} = 0.25$ mm, for which $f \in [0.55, 1.2]$ Hz; $A_{\text{wm}} = 0.5$ mm, for which $f \in [0.2, 1.0]$ Hz; and $A_{\text{wm}} = 1.0$ mm, for which $f \in [0.2, 0.5]$ Hz. The elongated shape of the wave maker allows the displacement of a large volume of fluid, producing long waves of small amplitude which have a negligible effect on the mean flow (we estimate the relative change in the Froude number v/c due to the passage of the wave to be at most 2%). The co-current waves thus excited were incident on the horizon; this is analogous to sending matter in towards a black hole from far away. The scattering process is illustrated in Figure 2. Much of the wave was simply transmitted (with amplitude T), while scattering at the effective potential also produced a reflected wave (with amplitude R) and a countercurrent wave in the supercritical region (with amplitude N).

Main results.—Focusing on the near-homogeneous regions (shaded gray in the lower right panel of Fig. 1), we assumed that the waveform in each is a sum of two plane waves, and were thus able to extract best-fit values for the amplitudes and wave vectors—see the Supplemental Material [31] for details. The subcritical region staying relatively flat over a considerable distance, we could take a longer near-homogeneous region there, and we thus expect greater accuracy of the results pertaining to this side.

Dispersion relation: In Figure 3 are shown the best-fit values of the wave vectors in each of the near-homogeneous regions. Immediately, we see that (with the exception of three outliers on the bottom right of the lower panel) each region shows two branches of the dispersion relation with clear signs of the derivative df/dk (where $f = \omega/2\pi$), this being the sign of the group velocity of the corresponding wave. We thus conclude that we have one ingoing and one outgoing wave on the subcritical side, while on the supercritical side we instead have two outgoing waves. This is indicative of the presence of an analogue black-hole horizon: it shows that $v - c$ changes sign when moving from one near-homogeneous region to the other.

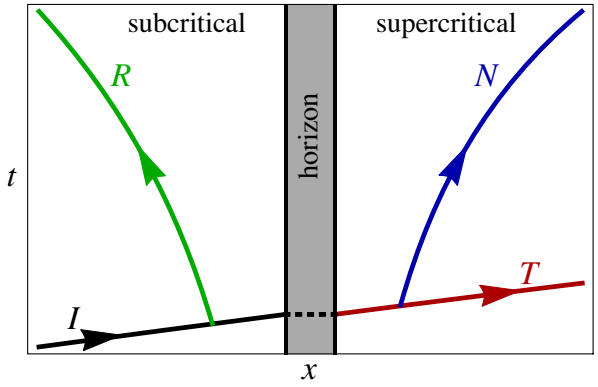

FIG. 2. Space-time diagram of the scattering process, showing the wave characteristics involved in the scattering of an incident co-current wave (I, black) into a transmitted co-current wave (T, red), a reflected countercurrent wave (R, green), and a transmitted countercurrent wave (N, blue). The flow is from left to right, passing from subcritical to supercritical.

Also shown are fits to the theoretical dispersion relations. As already mentioned, these take the linear form of Eq. (2) in the shallow-water regime $kh \ll 1$, so we may use the lower range of k to find the best-fit values of v and c in each region. These are given explicitly in Fig. 3; v is about 3% smaller than predicted by Eq. (3) (see the discussion below concerning the flow rate q), while c agrees with the prediction to within 0.1%. Moreover, since we expect the flow to be uniform in the subcritical region, we may use the best-fit values of v and c to find the corresponding values of q and h through Eqs. (3). Not only is the extracted water depth there, $h_{\text{sub}} = 56.7 \pm 0.1$ mm, consistent with the profile of Fig. 1, but it also agrees with the observed deviations from the linear dispersion relation [these dispersive corrections to the phase velocity are expected to take the form $c(k) = \sqrt{gh} \times \sqrt{\tanh{(hk)}/(hk)}$ [42], and are thus governed by the water depth h]. The fitted value of the flow rate is $q_{\text{fit}} = 143.6 \pm 0.3$ cm^2/s, which differs quite significantly from the measured value of 147.4 ± 0.7 cm^2/s. This is most likely due to the nonuniformity of the flow speed in the vertical direction. Indeed, numerical simulations indicate that v tends to decrease slightly near the surface, which would explain why q_{fit} is smaller than the measured value (see the Supplemental Material [31]).

On the supercritical side, the extracted wave vectors are considerably less accurate, having larger error bars and appearing to oscillate around the expected linear curves. While this is partly due to the reduction of the window size with respect to that in the subcritical region, it should be noted that there is a considerable degree of noise in the supercritical region. Even so, only four data points (which

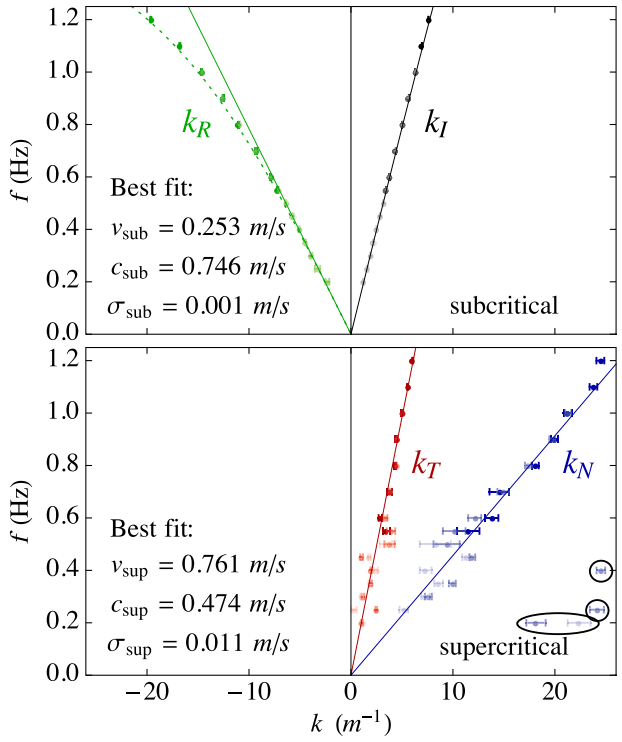

FIG. 3. Measured wave vectors. The various colors correspond to the modes of Fig. 2, while the three different shadings of data points correspond to different wave maker amplitudes: A_{wm} = 0.25 mm (dark), 0.5 mm (medium), and 1 mm (light). Circled points are outliers. The solid curves show theoretical dispersion relations fitted to the linear behavior of Eq. (2) for $kh \ll 1$. The fitted values of v and c in each region, as well as their error σ, are indicated. The dotted line in the upper panel shows the full theoretical dispersion relation with h_{sub} given by c_{sub} via Eqs. (3).

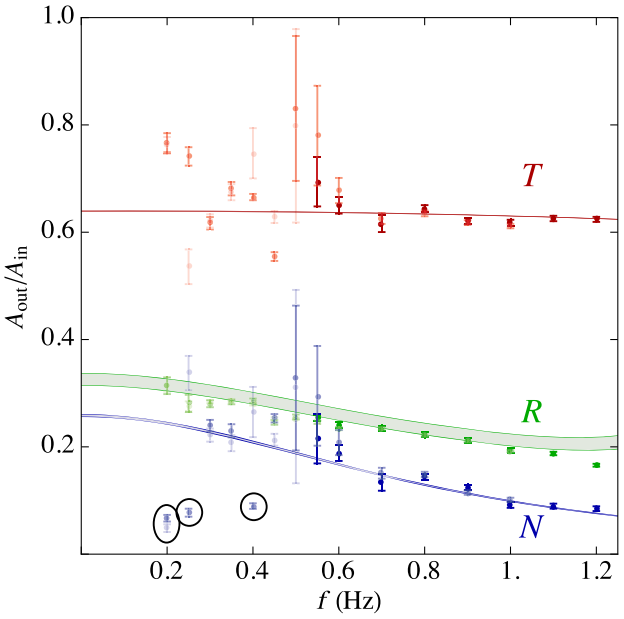

FIG. 4. Measured scattering amplitudes. The colors and shadings correspond to the same outgoing branches and wave maker amplitudes as in Fig. 3. The colored lines are theoretical predictions, and have finite widths corresponding to the uncertainty in h_{sub}. The amplitudes of the outliers circled in Fig. 3 are also circled here.

have been circled in Fig. 3) are clear outliers. v and c are found to be about 5 and 7% larger, respectively, than those predicted by Eqs. (3). This discrepancy is likely due to the nonuniformity of the flow after passing over the obstacle, and is reminiscent of a similar observation made in the downstream region in Ref. [21].

Scattering coefficients: In Figure 4 are shown the three outgoing wave amplitudes in units of the incident wave amplitude. Also shown are predictions extracted from the wave equation associated with the metric (1) [43]. As expected, the most accurate of the scattering amplitudes (in terms of the smallness of the error bars) is R, this having been extracted purely from the subcritical region. The amplitudes relating to the supercritical region are less accurately determined, with much larger error bars than R. This is due both to the smaller available window size where the flow is approximately homogeneous, and also to the presence of a significant amount of noise, which seems to be related to the occurrence of side wakes (see the Supplemental Material [31]). However, the extracted scattering amplitudes still compare favorably with the hydrodynamical theory.

In summary, we have extracted the dispersion relations and scattering amplitudes pertaining to the interaction of an incident co-current surface wave with an analogue black hole. The dispersion relations show a total of three outgoing modes, implying the presence of an analogue horizon. Except for the high-frequency sector of the R branch, the modes relevant to the scattering process are in the nondispersive regime where the effective metric description is valid, and the measured scattering amplitudes are compatible with its predictions.

Following in the spirit of [20,22], a future goal of this type of (classical) analogue model is the observation of (the stimulated version of) the Hawking process, whereby the squared norm of the relevant scattering coefficient takes the form of a thermal spectrum. The absence of transcriticality in previous experiments prevents the direct verification of the Hawking-Unruh thermal prediction, which can only be applied when a horizon is present. Our setup makes this possible in two ways. First, one could consider a stationary background like that used in this Letter. This can only be achieved by exploiting dispersion and sending in a short-wavelength mode [44], but these are difficult to excite in practice. The second possibility is to consider a time-dependent background in which an initially subcritical flow develops a supercritical region. In this context one can study, in particular, the scattering of initial long-wavelength countercurrent modes into final long-wavelength countercurrent modes (i.e., those labeled as R and N in the present work), thus avoiding the need to

send in a dispersive wave. This case is reminiscent of that originally studied by Hawking [4,5], of a star collapsing to form a black hole.

We would like to thank Romain Bellanger, Laurent Dupuis, and Jean-Marc Mougenot for their help concerning the experimental aspects of this work. We also thank Roberto Balbinot, Ulf Leonhardt, and particularly Florent Michel, Renaud Parentani, and Thomas Philbin for their careful reading of and constructive comments on a previous version of the manuscript. This work was supported by the French National Research Agency through Grant No. ANR-15-CE30-0017-04 associated with the project HARALAB, by the University of Poitiers (ACI UP on Wave-Current Interactions 2013–2014), by the Interdisciplinary Mission of CNRS which funded the linear motor of the wave maker in 2013, and by the University of Tours in a joint grant with the University of Poitiers (ARC Poitiers-Tours 2014–2015). It benefited from the support of the project OFHYS of the CNRS 80 Pprime initiative in 2019. It was partially supported by the Spanish Mineco Grants No. FIS2014-57387-C3-1-P and No. FIS2017-84440-C2-1-P, the Generalitat Valenciana Project No. SEJI/2017/042 and the Severo Ochoa Excellence Center Project No. SEV-2014-0398.

[1] C. Barceló, S. Liberati, and M. Visser, Analogue gravity, Living Rev. Relativity **14**, 3 (2011).
[2] C. Barceló, Analogue black-hole horizons, Nat. Phys. **15**, 210 (2019).
[3] W. G. Unruh, Experimental Black-Hole Evaporation?, Phys. Rev. Lett. **46**, 1351 (1981).
[4] S. W. Hawking, Black hole explosions?, Nature (London) **248**, 30 (1974).
[5] S. W. Hawking, Particle creation by black holes, Commun. Math. Phys. **43**, 199 (1975).
[6] T. G. Philbin, C. Kuklewicz, S. Robertson, S. Hill, F. König, and U. Leonhardt, Fiber-optical analog of the event horizon, Science **319**, 1367 (2008).
[7] F. Belgiorno, S. L. Cacciatori, M. Clerici, V. Gorini, G. Ortenzi, L. Rizzi, E. Rubino, V. G. Sala, and D. Faccio, Hawking Radiation from Ultrashort Laser Pulse Filaments, Phys. Rev. Lett. **105**, 203901 (2010).
[8] C. Ciret, F. Leo, B. Kuyken, G. Roelkens, and S.-P. Gorza, Observation of an optical event horizon in a silicon-on-insulator photonic wire waveguide, Opt. Express **24**, 114 (2016).
[9] J. Drori, Y. Rosenberg, D. Bermudez, Y. Silberberg, and U. Leonhardt, Observation of Stimulated Hawking Radiation in an Optical Analogue, Phys. Rev. Lett. **122**, 010404 (2019).
[10] H. S. Nguyen, D. Gerace, I. Carusotto, D. Sanvitto, E. Galopin, A. Lemaître, I. Sagnes, J. Bloch, and A. Amo, Acoustic Black Hole in a Stationary Hydrodynamic Flow of Microcavity Polaritons, Phys. Rev. Lett. **114**, 036402 (2015).
[11] J. Steinhauer, Observation of self-amplifying Hawking radiation in an analogue black-hole laser, Nat. Phys. **10**, 864 (2014).
[12] J. Steinhauer, Observation of quantum Hawking radiation and its entanglement in an analogue black hole, Nat. Phys. **12**, 959 (2016).
[13] J. R. M. de Nova, K. Golubkov, V. I. Kolobov, and J. Steinhauer, Observation of thermal Hawking radiation and its temperature in an analogue black hole, Nature (London) **569**, 688 (2019).
[14] R. Schützhold and W. G. Unruh, Gravity wave analogues of black holes, Phys. Rev. D **66**, 044019 (2002).
[15] G. Rousseaux, The basics of water waves theory for analogue gravity, in *Analogue Gravity Phenomenology: Analogue Spacetimes and Horizons, from Theory to Experiment*, edited by D. Faccio, F. Belgiorno, S. Cacciatori, V. Gorini, S. Liberati, and U. Moschella (Springer International Publishing, Cham, 2013), pp. 81–107, https://doi.org/10.1007/978-3-319-00266-8_5.
[16] P. R. Anderson, R. Balbinot, A. Fabbri, and R. Parentani, Hawking radiation correlations in Bose-Einstein condensates using quantum field theory in curved space, Phys. Rev. D **87**, 124018 (2013).
[17] P. R. Anderson, R. Balbinot, A. Fabbri, and R. Parentani, Gray-body factor and infrared divergences in 1D BEC acoustic black holes, Phys. Rev. D **90**, 104044 (2014).
[18] G. Rousseaux, C. Mathis, P. Maïssa, T. G. Philbin, and U. Leonhardt, Observation of negative-frequency waves in a water tank: A classical analogue to the Hawking effect?, New J. Phys. **10**, 053015 (2008).
[19] G. Rousseaux, P. Maïssa, C. Mathis, P. Coullet, T. G. Philbin, and U. Leonhardt, Horizon effects with surface waves on moving water, New J. Phys. **12**, 095018 (2010).
[20] S. Weinfurtner, E. W. Tedford, M. C. J. Penrice, W. G. Unruh, and G. A. Lawrence, Measurement of Stimulated Hawking Emission in an Analogue System, Phys. Rev. Lett. **106**, 021302 (2011).
[21] L.-P. Euvé, F. Michel, R. Parentani, and G. Rousseaux, Wave blocking and partial transmission in subcritical flows over an obstacle, Phys. Rev. D **91**, 024020 (2015).
[22] L.-P. Euvé, F. Michel, R. Parentani, T. G. Philbin, and G. Rousseaux, Observation of Noise Correlated by the Hawking Effect in a Water Tank, Phys. Rev. Lett. **117**, 121301 (2016).
[23] T. Torres, S. Patrick, A. Coutant, M. Richartz, E. W. Tedford, and S. Weinfurtner, Rotational superradiant scattering in a vortex flow, Nat. Phys. **13**, 833 (2017).
[24] L.-P. Euvé and G. Rousseaux, Classical analogue of an interstellar travel through a hydrodynamic wormhole, Phys. Rev. D **96**, 064042 (2017).
[25] A rotational vortex, as an analogue of a rotating $(2+1)$-dimensional spacetime with an ergoregion, has been realized in [23], but no mention is made of the possible presence of a horizon; note that dispersive models admit what may be termed "group velocity horizons" [1], i.e., turning points, but we use the term "horizon" in the more restrictive sense associated with the effective metric.
[26] F. Michel and R. Parentani, Probing the thermal character of analogue Hawking radiation for shallow water waves?, Phys. Rev. D **90**, 044033 (2014).

[27] S. Robertson, F. Michel, and R. Parentani, Scattering of gravity waves in subcritical flows over an obstacle, Phys. Rev. D **93**, 124060 (2016).
[28] A. Coutant and R. Parentani, Undulations from amplified low frequency surface waves, Phys. Fluids **26**, 044106 (2014).
[29] F. Michel, R. Parentani, and S. Robertson, Gravity waves on modulated flows downstream from an obstacle: The transcritical case, Phys. Rev. D **97**, 065018 (2018).
[30] J. Walker, The charm of hydraulic jumps, starting with those observed in the kitchen sink, Sci. Am. **244**, No. 4, 176 (1981).
[31] See the Supplemental Material at http://link.aps.org/supplemental/10.1103/PhysRevLett.124.141101 for a deeper theoretical treatment of the scattering process and further details on the data analysis, which includes Refs. [32–41].
[32] S. Robertson and G. Rousseaux, Viscous dissipation of surface waves and its relevance to analogue gravity experiments, arXiv:1706.05255.
[33] W. G. Unruh, Irrotational, two-dimensional surface waves in fluids, in Analogue Gravity Phenomenology: Analogue Spacetimes and Horizons, from Theory to Experiment, edited by Daniele Faccio, F. Belgiorno, S. Cacciatori, V. Gorini, S. Liberati, and U. Moschella (Springer International Publishing, Cham, 2013), pp. 63–80, https://doi.org/10.1007/978-3-319-00266-8_4.
[34] S. Corley and T. Jacobson, Hawking spectrum and high frequency dispersion, Phys. Rev. D **54**, 1568 (1996).
[35] J. Macher and R. Parentani, Black/white hole radiation from dispersive theories, Phys. Rev. D **79**, 124008 (2009).
[36] B. S. DeWitt, Quantum field theory in curved spacetime, Phys. Rep. **19**, 295 (1975).
[37] L. C. Baird, New integral formulation of the Schrödinger equation, J. Math. Phys. (N.Y.) **11**, 2235 (1970).
[38] S. Massar and R. Parentani, Particle creation and non-adiabatic transitions in quantum cosmology, Nucl. Phys. **B513**, 375 (1998).
[39] P. R. Anderson, A. Fabbri, and R. Balbinot, Low frequency gray-body factors and infrared divergences: Rigorous results, Phys. Rev. D **91**, 064061 (2015).
[40] F. Bouchon, T. Dubois, and N. James, A second-order cut-cell method for the numerical simulation of 2D flows past obstacles, Comput. Fluids **65**, 80 (2012).
[41] S. Osher and J. A. Sethian, Fronts propagating with curvature-dependent speed: Algorithms based on Hamilton-Jacobi formulations, J. Comput. Phys. **79**, 12 (1988).
[42] H. Lamb, *Hydrodynamics*, Dover Books on Physics (Dover Publications, New York, 1945).
[43] To improve the agreement between the theoretical prediction and the experimental data we have used refined versions of Eqs. (3) (see Eqs. (21) of the Supplemental Material [31]). We have also included dispersive corrections to the conversion factors relating normalized and "bare" amplitudes (see Eqs. (15) of the Supplemental Material [31]).
[44] There are two possibilities for the incident dispersive mode: either a short-wavelength gravity wave incident from the subcritical side, or a capillary wave travelling at "superluminal" speed with respect to the fluid and incident from the supercritical side; the conversion of capillary waves to long-wavelength gravity waves was demonstrated in the wormhole travel experiment [24], despite a high viscous damping rate for the capillary waves [32]